

Quantum Phase Transitions to Charge-Ordered and Wigner-Crystal States under the Interplay of Lattice Commensurability and Long-Range Coulomb Interactions

Yohei Noda and Masatoshi Imada

Institute for Solid State Physics, University of Tokyo, Kashiwanoha, Kashiwa, Chiba 277-8581, Japan

(Received 26 February 2002; published 8 October 2002)

The relationship among the Wigner crystal, charge ordering, and the Mott insulator is studied by the path-integral renormalization group method in two-dimensional systems with long-range Coulomb interaction. In contrast to the insensitivity of the Hartree-Fock results, the stability of the solid drastically decreases with the decrease in the lattice commensurability. The transition to liquid occurs at the electron gas parameter $r_s \sim 2$ for the filling $n = 1/2$, showing a large reduction from $r_s \sim 35$ in the continuum limit. A correct account of quantum fluctuations is crucial to understanding the charge-order stability generally observed only at simple fractional fillings and the nature of quantum liquids away from them.

DOI: 10.1103/PhysRevLett.89.176803

PACS numbers: 73.20.Qt, 71.10.Ca, 71.10.Fd, 71.30.+h

Coulomb interaction drives various types of electron crystallization ranging from Wigner lattice, charge-order including stripes to Mott insulator. The Wigner transition in the continuum space was studied on two-dimensional (2D) electron systems by quantum Monte Carlo calculations and the transition point was estimated to be $r_s \sim 35$ at zero temperature [1,2], where $r_s = r_0/a_B$ with the Wigner Seitz radius $r_0 = 1/\sqrt{\pi n_e}$, the Bohr radius $a_B = 4\pi\epsilon\hbar^2/m^*e^2$, and the electron density n_e . This transition in the quantum region was experimentally realized in GaAs heterostructure at $r_s \sim 35$ in good agreement with the theoretical prediction [3].

The most dramatic effect of atomic periodic potential in crystal not contained in the electron gas is apparently the band formation in electronic spectra due to Bloch theorem. In this Letter, we stress another crucial concept, lattice commensurability, generates another dramatic effect of the periodic potential when the Coulomb interaction is present. In correlated electron systems, as in transition metal compounds [4,5] and organic systems [6], charge-ordering phenomena including stripe type are common when the electron filling n satisfies simple fractional number such as $1/2$ and $1/3$. These phenomena have attracted much interest in relation to the mechanisms of high- T_c superconductivity in the cuprates and colossal magnetoresistance in the manganites. However, in those systems, as we discuss later, the effective value of r_s is usually estimated to be rather small in the range $r_s < 10$, though we have some uncertainty for the estimate of the effective mass m^* and the dielectric constant ϵ . At such low values of r_s , we expect the quantum melting of electrons in terms of the above electron gas picture. When n deviates from a simple fractional number, such charge orders indeed usually melt to metals or the charge periodicity is pinned at the simple fillings with added carriers localized by disorder. It implies that a mechanism of stabilizing the solid only at simple commensurate fillings works very efficiently. The Mott insulator can be viewed

as the extreme limit of strong commensurability, which can be stabilized even at lower effective r_s with a common incompressible nature.

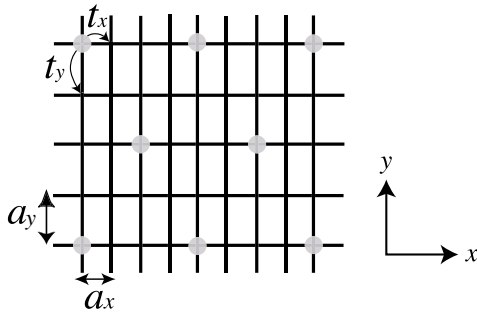
In this Letter, we show that the mechanism for such common stabilization of the solid only at simple fractional fillings is puzzling in the Hartree-Fock (HF) calculations, whereas it can indeed be understood only when the quantum many-body fluctuation effects are seriously considered. We also show that a simple metal *ala* the band theory actually has a complex hierarchy structure of charge-order insulators and their proximities.

We employ a Hamiltonian given as

$$\hat{H} = \hat{H}_0 + \hat{H}_I, \quad \hat{H}_0 = - \sum_{\langle i,j \rangle, \sigma} t_{ij} (c_{i\sigma}^\dagger c_{j\sigma} + \text{H.c.}),$$

$$\hat{H}_I = U \sum_i n_{i\uparrow} n_{i\downarrow} + \frac{1}{2} \sum_{i \neq j} V_{ij} n_i n_j, \quad (1)$$

where the notations follow the standard one in the Hubbard-type models. We take the long-ranged Coulomb term as $V_{ij} = V/|r_i - r_j|$, where we ignore possible screening arising from electrons in other bands. The jellium model is employed by assuming a uniform positive-charge background while the effect of ionic periodic potential is represented by the lattice with single-band electrons located near the Fermi level. The on site interaction U measured from V may depend on the detailed structure of atomic orbitals. Here we take $U/t = 4$ throughout this paper for simplicity. This ratio may be more or less the lower bound for the real situations. In any case, our results in this Letter for $n \leq 1/2$ do not sensitively depend on this ratio. Effects of U become relevant for the Mott insulator ($n = 1$), which are discussed in more detail in a separate paper [7]. Here, we study spinless fermion models in addition to spin- $1/2$ electrons. This corresponds to the fully polarized ferromagnetic case. We impose the periodic boundary condition in our numerical studies. The Coulomb interactions between

FIG. 1. Lattice structure with anisotropic transfers t_x and t_y .

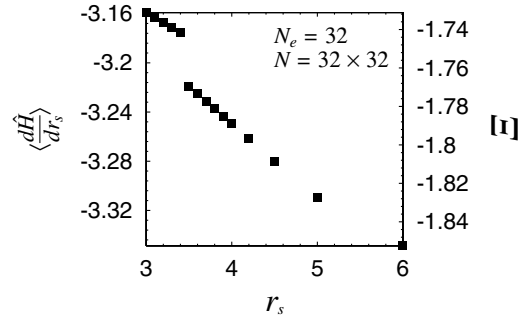
images across the periodic boundaries are taken by the Ewald summation.

Since our purpose in this Letter is to understand a generic and universal feature of the interplay between quantum fluctuations and commensurability, we restrict our study to the 2D rectangular lattice with the anisotropy of lattice constants a_x and a_y as well as t_x and t_y taken as simple as possible to avoid a possible complexity which may intervene the clarification of the essence. The transfer is limited to the nearest-neighbor pairs in x and y directions denoted by t_x and t_y as in Fig. 1. The anisotropy $d = a_y/a_x$ is chosen to make the charge ordering with a right triangular lattice structure possible at the given filling. By this choice, the commensurability effect can be solely extracted and can be compared on the same grounds with the continuum limit, because the same structure is found in the continuum limit. To see a systematic dependence on r_s , we control t_x and t_y by a single parameter of the effective mass m^* as $t_z = \hbar^2/2m^*a_z^2$ with $z = x$ or y , which reproduces the dispersion in the continuum limit and enables the comparison of low-filling results with the continuum limit. The effects of specific anisotropies do not change our main results on the commensurability effects.

The above Hamiltonian may be rewritten as $\hat{H}_R = \hat{H}_0 + \hat{H}_I$, $\hat{H}_0 = -[d/(\pi n r_s^2)] \sum_{\langle i,j \rangle, \sigma} (c_{i\sigma}^\dagger c_{j\sigma} + \text{H.c.}) - [1/(\pi d n r_s^2)] \sum_{\langle i,j \rangle, \sigma} (c_{i\sigma}^\dagger c_{j\sigma} + \text{H.c.}) + [2/(\pi n r_s^2)] (d + \frac{1}{d}) \hat{N}_e$, $\hat{H}_I = U \sum_i n_{i\uparrow} n_{i\downarrow} + \sqrt{d/(\pi n)} \frac{1}{r_s} \sum_{i,j} [(n_i n_j)/(|\mathbf{r}_j - \mathbf{r}_i|)]$ in the energy unit of Rydbergs, where \hat{N}_e is the total electron-number operator. By the continuum limit of vanishing a_x and a_y and $n \rightarrow 0$, with r_s fixed, the above Hamiltonian is reduced to that of conventional electron gas.

We first discuss the HF calculation for spinless fermions. For $n < 1/2$, the first-order transitions are clearly visible from the jump of $\langle d\hat{H}/dr_s \rangle$, e.g., in Fig. 2 at $r_{sc} = 3.45 \pm 0.05$ for $n = 1/32$ on the 32×32 lattice. The jump indicates the level crossing as a function of r_s . The right ordinate is the scale for the second Hamiltonian \hat{H}_R defined by $\Xi = \partial(r_s^2 \hat{H}_R)/\partial r_s = (d/\pi n) \partial \hat{H}/\partial r_s$. The crystallization is indeed identified in the two-body correlation defined by $C(\mathbf{r}_i) = \frac{1}{N} \sum_{\mathbf{r}_j} \langle n_{\mathbf{r}_j + \mathbf{r}_i} n_{\mathbf{r}_j} \rangle$ in Fig. 3,

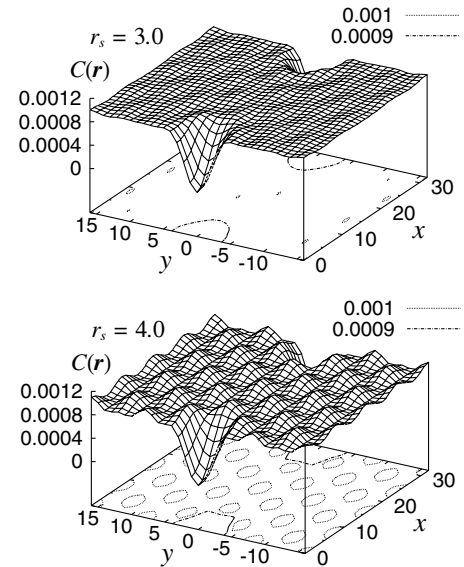
For fixed electron-number N_e , the transition point is first extrapolated to the continuum limit $n \rightarrow 0$ and then

FIG. 2. Hartree-Fock result for dH/dr_s vs r_s for 32 spinless electrons on 32 by 32 lattices.

to the thermodynamic limit $N_e \rightarrow \infty$ as in Fig. 4. The small size dependence suggests that $N_e = 8$ gives already a good estimate of the thermodynamic limit. At $n = 1/2$, the transition is of continuous type with the absence of a jump in $\langle dH/dr_s \rangle$ while the Fourier transform of two-body charge correlation diverges at the peak as a Bragg peak with increasing system size for $r_s \geq r_{sc}$. The transition is at $r_{sc} = 0.9 \pm 0.1$ after finite-size scaling.

Spin-1/2 electrons are also analyzed at $n = 1/4$ and $1/2$. The transitions appear to be of first order at $r_{sc} = 2.05 \pm 0.05$ and continuous at $r_{sc} = 1.35 \pm 0.15$, respectively. The orders of transitions are the same as the spinless case and the difference of r_{sc} between these two cases shrinks with decreasing filling. The HF approximation predicts the crystallization of 2D electrons ranging from $r_{sc} \sim 1$ at $n = 1/2$ to $r_{sc} \sim 3.69$ in the continuum limit. The filling dependence is rather small.

To understand how quantum and many-body fluctuations modify the HF results, we have calculated the

FIG. 3. Hartree-Fock result for two-body correlation function for 32 spinless electrons on 32 by 32 lattice. The periodic structure for $r_s = 4.0$ indicates long-range order with the triangular lattice structure while it is absent at $r_s = 3.0$.

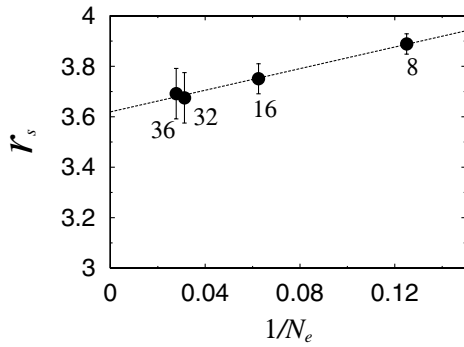


FIG. 4. The Hartree-Fock results for liquid-solid transition points of spinless electrons as a function of the inverse of the particle number N_e in the limit $n \rightarrow 0$.

ground state of this system by applying the path-integral renormalization group (PIRG) method [8]. By following the path-integral formalism, the long-ranged Coulomb term is rewritten by using the Stratonovich-Hubbard transformation [9]. We took the number of nonorthogonal Slater determinant basis, L , up to 256 and extrapolated as a function of the energy variance, where the zero variance limit gives an exact ground-state estimate in the full Hilbert space. Below, we show results when the extrapolation linearly converges well. Figure 5 shows typical examples of the extrapolation for $\langle dH/dr_s \rangle$. We note that the HF result is nothing but that at $L = 1$ in PIRG and the quantum many-body fluctuations are taken into account systematically with increasing L . Typically, the energy variance at the largest L is 1 order of magnitude smaller than that at $L = 1$.

We took lattice sizes up to 144 sites (12×12 lattice) with electrons up to 72 at quarter filling $n = 1/2$ for both spinless and spin-1/2 electron systems. At $n = 1/8$ and $1/18$, we show only on the spinless system for 64 and 144 sites, respectively, with eight electrons. We restricted to the spinless case for these low fillings since the difference from that with spins is estimated to be small. This is inferred from the comparisons of the PIRG with the HF results at $n = 1/2$ together with the HF results at lower filling with spins. In fact, the spin effects appear mainly

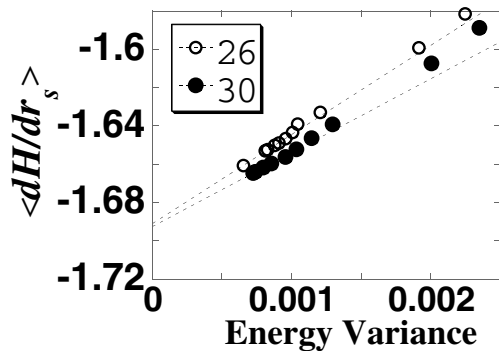


FIG. 5. The extrapolation of $\langle dH/dr_s \rangle$ with the energy variance at $r_s = 26$ (open circles) and 30 (closed circles) for the case of Fig. 6.

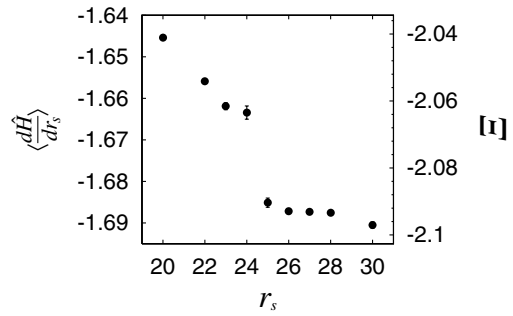


FIG. 6. PIRG result for dH/dr_s vs r_s for eight spinless electrons on 12 by 12 lattices.

through the exchange process. The exchange is scaled by t^2 , where t is the effective transfer between neighboring electrons. At lowering fillings, it forms lower-energy hierarchy than that of the charge order, V . Though spin is important in determining the magnetic order, this small energy scale hardly changes the solid-liquid transition for $n \leq 1/2$. The system-size dependence of the transition appears to be small at the low fillings because the transition becomes first order. Therefore, though our systems at the low fillings are rather small, the results are expected to be close to the thermodynamic ones.

We first show spinless cases. Figure 6 shows a typical example showing the first-order transition in the PIRG calculation at $n = 1/18$ for eight fermions on a 12 by 12 lattice. The jump is similar to the HF results with a clear change of the correlation as in Fig. 7. However, the transition takes place at substantially higher r_s than the HF result. The transition at $n = 1/8$ is also first order while that seems to be of continuous type again at $n = 1/2$. The transition is estimated to be at $r_{sc} = 1.75 \pm 0.25$, 13.5 ± 0.5 , and 24.5 ± 0.5 for $n = 1/2$,

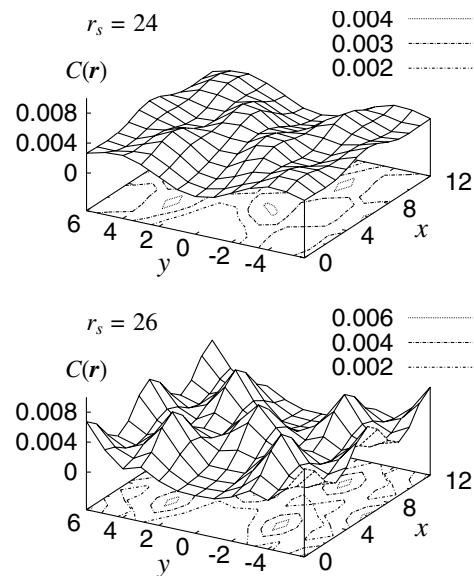


FIG. 7. PIRG result for two-body correlation function for eight spinless electrons on 12 by 12 lattice.

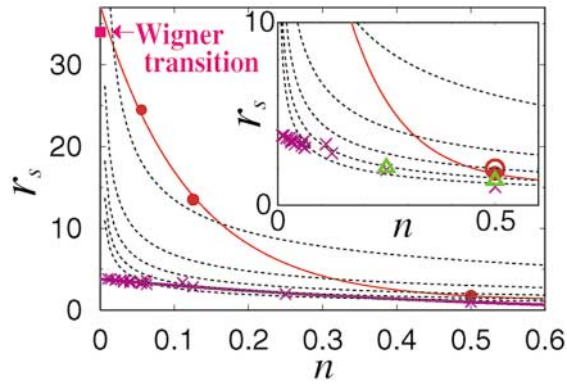


FIG. 8 (color). Solid-liquid phase boundary in plane of the filling $n = 1/l$ and r_s . The square indicates the Wigner transition point [1]. The PIRG results (filled and open circles for spinless and spin-1/2 fermions, respectively) are compared with the Hartree-Fock results (crosses for spinless and triangles for spin-1/2 electrons). The solid curves are guides for the eye for the envelope of the boundary at $n = 1/l$. The dotted curves show contour lines for the ratio of ϵ/m^* to the bare value being at 1, 2, 3, 4, and 5 from up to down. The inset enlarges the small r_s region.

1/8, and 1/18, respectively. We have also studied spin-1/2 electrons at $n = 1/2$ and obtained a continuous transition at $r_{sc} = 2.0 \pm 1.0$, which is comparable to the spinless case.

In Fig. 8, the solid-liquid phase boundary, r_{sc} , is shown and the HF and PIRG results are compared for $n = 1/l$ with integer l . From the plot, r_{sc} appears to form a smooth envelope for $n = 1/l$. At simple fractional filling such as $n = 1/2$, r_{sc} by the HF approximation is relatively good. However, it deviates from the PIRG results rapidly with increasing l . The ratio of these two estimates increases from ~ 1.5 – 2 at $n = 1/2$ to ~ 10 in the continuum limit. In terms of the electron density, this difference means from 3–4 to 100, since the density is scaled by r_s^2 . From the PIRG results, we can understand why charge orders are commonly observed in organic and transition metal compounds at simple fractional fillings as 1/3, while it is pinned or melts away from such fillings because r_{sc} increases dramatically with an increasing denominator of the irreducible fraction while the parameters of many compounds may lie in this range of variations. For example, when we assume a layered perovskite structure with the lattice constant $a = 4 \text{ \AA}$ and the effective ratio ϵ/m^* being twice the bare value, $n = 1/2$, $1/3$, and $2/3$ are within the solid region while $n = 1/4$, $3/4$, and fractions with higher denominators are in the liquid region as in Fig. 8. We note that the filling control at fixed lattice constants follows a contour line of ϵ/m^* in Fig. 8. We also see that the HF approximation qualitatively fails in accounting this general experimental trend.

With increasing m^*/ϵ , the charge-order states may form “devil’s staircase” when r_s approaches 35, since fillings at irreducible fractions with the same denomina-

tor may have similar r_{sc} . Competitions with hierarchical structure formation by various levels of fractional fillings are also expected. Even metallic states near the charge order may contain charge-order proximities when the static solid could be stabilized on the mean-field level. In this context, for $n = 1/l$ with decreasing integer l , the charge-order transition becomes a more continuous type, which must accompany larger quantum fluctuations. This may be particularly conspicuous near the simple commensurate order such as the Mott insulator [7]. Re-analyses of mechanisms of high- T_c superconductivity in the cuprates and the colossal magnetoresistance in the manganites from the present insight would be a future intriguing issue, since they appear in the proximity of insulator stabilized by the simple commensurability.

In summary, we have studied the liquid-solid transition of two-dimensional electrons with long-range Coulomb interaction. We have shown how the Mott insulator at $n = 1$, charge orders at $0 < n < 1$, and the Wigner lattice at $n \rightarrow 0$ are connected. The charge-order transition does not sensitively depend on the spin degrees of freedom for $n < 1/2$. Although the HF transition points are rather insensitive to the electron filling and lattice commensurability, the PIRG result with quantum fluctuations taken in a correct way shows a rapid increase of r_s for the transition when the commensurability becomes weak. The present PIRG results explain why charge orders or stripes are commonly observed only at simple fractional fillings such as 1/2 and 1/3 but are not away from them. We stress that such interplay between quantum fluctuations and the commensurability may play a crucial role also in metals (quantum liquids). It would be interesting if the interplay can be experimentally studied by micro-fabrication of periodic potential to 2D electron systems.

The work is supported by JSPS under Grant No. JSPS-RFTF97P01103. A part of the computation was done at the supercomputer center at ISSP, University of Tokyo.

- [1] M. Imada and M. Takahashi, J. Phys. Soc. Jpn. **53**, 3770 (1984).
- [2] B. Tanatar and D. M. Ceperley, Phys. Rev. B **39**, 5005 (1989).
- [3] J. Yoon *et al.*, Phys. Rev. Lett. **82**, 1744 (1999).
- [4] For a review, see M. Imada, A. Fujimori, and Y. Tokura, Rev. Mod. Phys. **70**, 1039 (1998).
- [5] J. M. Tranquada, J. Phys. Chem. Solids **59**, 2150 (1998).
- [6] For example, K. Hiraki and K. Kanoda, Phys. Rev. Lett. **80**, 4737 (1998).
- [7] T. Kashima and M. Imada, J. Phys. Soc. Jpn. **70**, 3052 (2001); H. Morita, S. Watanabe, and M. Imada, J. Phys. Soc. Jpn. **71**, 2109 (2002).
- [8] M. Imada and T. Kashima, J. Phys. Soc. Jpn. **69**, 2723 (2000); T. Kashima and M. Imada, J. Phys. Soc. Jpn. **70**, 2287 (2001).
- [9] Y. Noda and M. Imada (unpublished).